HDACi vorinostat protects muscle from degeneration after acute rotator cuff injury in mice

Cite this article:
Bone Joint Res 2024;13(4):
169–183.

DOI: 10.1302/2046-3758.
134.BJR-2023-0292.R1

Correspondence should be sent to Ana Pérez-Ruiz
aperu@unav.es

L. Gil-Melgosa,[1] R. Llombart-Blanco,[1] L. Extramiana,[2] I. Lacave,[3] G. Abizanda,[2] E. Miranda,[4] X. Agirre,[4] F. Prósper,[4,5,6] A. Pineda-Lucena,[7] J. Pons-Villanueva,[1] A. Pérez-Ruiz[2]

[1]Orthopedic Surgery Department of Clínica Universidad de Navarra (CUN) and Instituto de Investigación Sanitaria de Navarra (IdiSNA), Pamplona, Spain
[2]Technological Innovation Division, Foundation for Applied Medical Research (FIMA), University of Navarra (UNAV) and IdiSNA, Pamplona, Spain
[3]Clinica Universidad de Navarra, Pamplona, Spain
[4]Hemato-Oncology Program, FIMA-UNAV and IdiSNA, Pamplona, Spain
[5]Haematology Department, Clinica Universidad de Navarra, Pamplona, Spain
[6]Centro de Investigación Biomédica en Red en Bioingeniería, Biomateriales y Nanomedicina (CIBER-BBN), Madrid, Spain
[7]Medicinal Chemistry Program, FIMA-UNAV and IdiSNA, Pamplona, Spain

Aims

Rotator cuff (RC) injuries are characterized by tendon rupture, muscle atrophy, retraction, and fatty infiltration, which increase injury severity and jeopardize adequate tendon repair. Epigenetic drugs, such as histone deacetylase inhibitors (HDACis), possess the capacity to redefine the molecular signature of cells, and they may have the potential to inhibit the transformation of the fibro-adipogenic progenitors (FAPs) within the skeletal muscle into adipocyte-like cells, concurrently enhancing the myogenic potential of the satellite cells.

Methods

HDACis were added to FAPs and satellite cell cultures isolated from mice. The HDACi vorinostat was additionally administered into a RC injury animal model. Histological analysis was carried out on the isolated supra- and infraspinatus muscles to assess vorinostat anti-muscle degeneration potential.

Results

Vorinostat, a HDACi compound, blocked the adipogenic transformation of muscle-associated FAPs in culture, promoting myogenic progression of the satellite cells. Furthermore, it protected muscle from degeneration after acute RC in mice in the earlier muscle degenerative stage after tenotomy.

Conclusion

The HDACi vorinostat may be a candidate to prevent early muscular degeneration after RC injury.

Article focus

- This study focuses on muscle degeneration/regeneration after a rotator cuff (RC) injury through exposure to the histone deacetylase inhibitor (HDACi) vorinostat in an animal model.

Key messages

- Epigenetic control of fibro-adipogenic progenitors (FAPs) within the muscle, and their interaction with satellite cells, may influence muscle degeneration following early RC injury.

Bone & Joint Research

Strengths and limitations

- We studied a therapeutic approach for RC injuries by administering the HDACi vorinostat, considering the two main cell populations responsible for disease progression and regeneration: FAPs and satellite cells.
- The potential therapeutic effects of HDACi vorinostat in the early-to-middle stages of RC injury are lost in the latter stages of the disease. However, we did not analyze extended drug exposure after RC injury.

Introduction

Rotator cuff (RC) injuries are common in the shoulder and typically involve tears or damage to one or more of the tendons, most commonly the supraspinatus tendon. These injuries can occur due to acute trauma, repetitive strain, or degenerative changes over time, with the prevalence of tear increasing dramatically with age. RC injuries mostly result in muscle degeneration, which further exacerbates functional impairment in the shoulder.[1] Development of muscular fatty infiltration is one of the major triggers of RC injury progression.[2] In recent research, the role of fibro-adipogenic progenitors (FAPs) and their interaction with the satellite cells have gained attention as key players in this deleterious process.

FAPs and satellite cells are two distinct cell populations within the skeletal muscle that play important roles in muscle regeneration and repair. FAPs are a population of multipotent cells located in the skeletal muscle interstitium with the ability to differentiate into both fibroblasts and adipocytes, contributing to the pathological processes of muscle degeneration, fibrosis, and fatty infiltration.[3-5] Satellite cells, on the other hand, are a population of non-interstitial muscle stem cells located beneath the basal lamina of muscle fibres, whose mission is to maintain the haemostatic condition of the skeletal muscle by providing myogenic cells, and replenishing the stem cell compartment when required.[6-8] The presence of activated FAPs, and the altered microenvironment they create after tendon injury, influence the behaviour and fate of satellite cells through paracrine signalling and cell-cell interactions, thereby affecting muscle repair and further compromising tissue quality and function.[9-12] Understanding the interplay between FAPs, satellite cells, and other cell types in the injured RC tissue is essential for unravelling the mechanisms of muscle degeneration and regeneration. Furthermore, targeting FAPs and modulating their behaviour, as well as promoting satellite cell activation and function, may hold therapeutic potential for providing muscle repair and improving functional outcomes in RC injuries.[13]

Histone deacetylase inhibitors (HDACis) are a class of epigenetic compounds that interfere with the activity of histone deacetylases (HDACs). HDACis prevent the removal of acetyl groups from histone proteins, resulting in a more relaxed chromatin structure and increased gene expression. Different HDACis have shown promise in various biological processes, including their beneficial effects in treating muscle atrophy and degeneration, at least partially through their impact on FAPs.[14-16] Therefore, HDACis represent a promising agent for the development of muscle-specific therapeutics in the future. However, the use of HDACis in clinical settings is still in the early stages, and more research is needed to fully understand their efficacy, safety, and potential side effects in the context of skeletal muscle.

Here, we examined the effect of different available HDACis on FAPs and satellite cells isolated from muscles of wild-type mice, including: entinostat, a class I HDAC-selective HDACi; vorinostat, a pan-HDACi also known as suberoylanilide hydroxamic acid (SAHA); and quisinostat, a second-generation hydroxamate-based pan-HDACi with stronger potency towards class I HDAC. From its effect on the in vitro phenotype of these muscle-associated stem cell populations, we further tested the role of HDACi vorinostat in regulating muscle degeneration in a mouse massive RC tear model, hypothesizing that it can inhibit FAP adipogenesis and promote satellite cell recruitment to reduce muscle degeneration in the earlier stage of RC injury.

Methods

Animal procedures

Four male and female wild-type C57BL/6 J mice (Envigo, UK; Ref. 057) aged eight weeks were killed by cervical dislocation to isolate FAPs and satellite cells (Supplementary Figure a). Three males and females were killed at the age of 12 weeks and were used as healthy controls (Supplementary Figure a). Additionally, 16 male and 16 female mice underwent unilateral massive RC tear surgery at 12 weeks of age, and were subjected to complete supraspinatus and infraspinatus tendon transection and suprascapular denervation transection. A total of 12 injured animals were killed two, 14, and 28 days after RC injury, while 20 injured mice received vorinostat or control treatment two days after tenotomy and were killed 12 or 26 days later (Supplementary Figure a). Surgical procedures were carried out under 2% isoflurane inhalation anaesthesia (Isovet; Braun, Germany) with aseptic conditions and optical magnification (SZ61; Olympus, Japan). The left upper limb of the mice was shaved and disinfected with chlorhexidine. A longitudinal incision was made lateral to the distal part of the shoulder to the humeral head, and a careful dissection exposed the deltoids to visualize the supra and infraspinatus tendons. A complete tenotomy was performed in both tendons. Additionally, the suprascapular nerve was also dissected after its localization under the trapezius muscle. Antibiotic prophylaxis with subcutaneus 10 mg/kg enrofloxacin (Baytril 2.5%; Bayer, Germany) and intraperitoneal analgesic medication with 300 µg/kg fentamyl (Fentanest; Kern Pharma, Spain) and subcutaneous 5 mg/kg meloxicam (Metacam; Boehringer Mannheim, Germany) were administered to all specimens before and after surgery. The animals were kept in cages with environmental enrichment, with access to food and water ad libitum. Weekly, they were examined and weighed to check their correct development. All animal procedures performed in this study were subjected to the Directive 2010/63/EU of the European Parliament and Council on the protection of animals used for scientific purposes, and the Real Decreto RD53/2013 (protocol number 039-18). The veterinarian and the surgical team members (GA, IL, LGM, RLB, JPV) identified the experimental groups by using a punch code number in the mice's ears, labelling the animal cages with identification letters. These codes were later associated with a code number to identify the origin of any muscle under study. The authors have adhered to the ARRIVE

guidelines for animal studies, and have included an ARRIVE checklist in the Supplementary Material.

FAPs and satellite cells isolation and culture

The hind limb muscles of wild-type mice were isolated and mechanically disaggregated and dissociated in Ham's F10 media containing collagenase II 0.2% (Worthington)/$CaCl_2$ (Sigma-Aldrich, USA; 2.5 mM) at 37°C for 30 minutes followed by a digestion with collagenase D (Roche; 1.5 U/ml)/Dispase (Roche; 1 U/ml) at 37°C for 60 minutes. Cells were incubated in lysing buffer (BD Pharm Lyse) for ten minutes on ice and re-suspended in phosphate-buffered saline (PBS) with 2.5% goat serum. FAPs were isolated from muscle-associated cell populations by using fluorescein isothiocyanate (FITC)-conjugated anti-Sca-1 antibody (BioLegend, USA; 108113/14), while Alexa647-conjugated anti-CD34 (BD Pharmingen, USA; 560230) and phycoerythrin (PE)-conjugated anti-α7-integrin (AbLab, Canada; 53-0010-05; clone R2F2) antibodies were used for double positive staining of quiescent satellite cells. Lineage-negative (Lin^-) cells, detected by PE-Cy7-conjugated anti-CD45 (BioLegend 103113/14), anti-CD31 (BioLegend 10241/8), and anti-CD11b (BioLegend 101215/16) antibodies, were discarded. Cells were sorted using a FACS Aria II flow cytometer (BD) by following the gating strategy shown in Supplementary Figures ba to be. FAPs and satellite cells were cultured in mitogen-rich media (Dulbecco's modified Eagle's medium (DMEM) with 20% foetal bovine serum (MilliporeSigma, USA), 10% horse serum (Gibco; Thermo Fisher Scientific, USA), 1% chick embryo extract (ICN Flow), 2 mM L-glutamine, and 1% penicillin-streptomycin), in culture plates coated with 1 mg/ml Matrigel (Corning) at 37°C in 5% CO_2. Purity of sorted cells was analyzed by quantitative polymerase chain reaction (qPCR) and immunostaining during their in vitro differentiation (Supplementary Figures bf to bl).

Drug treatment

For the in vitro studies, entinostat (a HDACi selective for class I HDAC), vorinostat (SAHA, a pan-HDACi), and quisinostat (a hydroxamate-based second-generation pan-HDACi with stronger potency toward class I HDAC) were prepared in DMSO as a solvent, diluted in PBS, and added daily to the FAPs for five consecutive days (Supplementary Figure ca). A similar procedure was carried out in the satellite cells (Supplementary Figure cb), this time maintaining the cells for six days. Additionally, a group of satellite cells that received the supernatant of FAPs, which had been treated with the epigenetic compounds 24 hours previously, was included (Supplementary Figure cc). In parallel, vehicle-treated groups (controls) received saline plus an equivalent amount of DMSO solvent diluted in PBS. Each experiment was carried out in duplicate using three independent biological samples, and each sample was assigned a code number for blind analysis.

For the in vivo studies, a daily dose of vorinostat (5 mg/ml) in Tween-saline buffer was intraperitoneally injected into the RC injured mice during 12 or 26 days, 48 hours after tenotomy. Control-injured mice received the same volume of HDACi-diluent. Vorinostat was well tolerated by the RC-injured mice, and did not cause noticeable side effects or signs of toxicity, including weight reduction, hyperexcitability, or sudden death. This dose has been used previously in a muscular dystrophy mouse model, and evidence of both recovery in muscle strength and improvements in histology was observed.[17]

Muscle processing and immunostaining

Skeletal muscles were assigned a code number for blinded analysis. Sections were fixed for five minutes in 4% paraformaldehyde and treated in 20% sucrose at 4°C overnight. Then, muscle tissues were frozen in optimal cutting temperature compound cooled in dried ice, and serial 8 transversal cryosections of 9 μm thickness were collected at 400 μm intervals through the entire infraspinatus and supraspinatus muscles of each animal. Sections were additionally fixed in 10% formalin for 20 minutes and rinsed in PBS. When required, tissue sections were permeabilized with 0.1% Triton X-100/PBS, citrate buffer or 0.2% Trypsin/$CaCl_2$, and blocked. The following primary antibodies were applied (4°C, overnight): mouse anti-Pax7, anti-MyHC (clone MF-20), anti-MyHC type IIA (clone SC-71), anti-MyHC type IIB (clone BF-F3), anti-MyHC type IIX (clone 6H1) (Developmental Studies Hybridoma Bank (DSHB), USA), anti-CD31 (BD Pharmigen), anti-αSMA-Cy3 (Sigma-Aldrich), rat anti-Ki67 (eBioscience; Thermo Fisher Scientific), anti-CD45 (BioLegend), goat anti-PDGFRα (eBioscience), rabbit anti-laminin (Sigma-Aldrich), anti-perilipin, and anti-H3Ac (Cell Signaling Technology, USA) antibodies. Primary antibodies were visualized with fluorochrome-conjugated secondary antibodies (goat/donkey anti-mouse-488/594/647 and/or goat/donkey anti-rabbit-488/594/647 and/or goat anti-rat-594/647; Molecular Probes, USA) or with biotin-labelled secondary antibodies followed by tyramide signal amplification kit, before mounting in faramount fluorescent mounting medium containing 4',6-diamidino-2-phenylindole (DAPI; 100 ng/ml; Molecular Probes).

Digital image acquisition and quantification

Immunostained cells and muscle tissue sections were viewed using a Zeiss Axiophot epifluorescence microscope (Zeiss, Germany). Digital images were acquired with an AxioCamMR3 (Zeiss) and processed using Fiji software. When needed, images were composed and edited, and modifications were applied to the whole images using Photoshop CS6 (Adobe, USA).

Images of immunostained cells were taken (10×) in 20 independent fields from two different wells of each cell condition, maintaining the same image acquisition conditions. Experiments were performed in triplicate. In immunostained muscle tissue sections, tile-stacks of perilipin (fatty infiltration), CD45 (inflammation), CD31 (small vessels), and CD31/αSMA (large vessels) were captured (10×) from eight serial cryosections of the supra and infraspinatus muscles of each animal. Positive staining was expressed as the percentage of the stained area divided by the total area of muscle. $Pax7^+$, $Pax7^+Ki67^+$, and $Pax7^+Ki67^-$ satellite cells were counted in two whole muscle sections from each animal in at least four animals per group and related to the area of the muscle. $PDFGR\alpha^+$ cells were counted in 15 to 20 different captures (63×) from two whole muscle sections from each animal. Z-stacks of $Pax7^+Ki67^{+/-}H3Ac^+$ and $PDFGR\alpha^+H3Ac^+$ cells were acquired (63×), fixing shutter speed. Quantification of H3Ac mean intensity was performed by using a plugin developed for Fiji/ImageJ (National Institutes of Health, USA). Morphometry determined the cross-sectional area (CSA;

μm²) of each muscle or fibre after laminin immunostaining. Tile-stacks captures (10×) from two different tissue sections of at least four animals were analyzed. Fibre-type composition of infra- and supraspinatus muscles was calculated by manually counting the total number of fibres (type IIA, IIB, and IIX) from two different tissue sections of three healthy mice and related to the total area of each section. Then, the percentage of each fibre type was calculated considering the total number of laminin-stained fibres as 100%.

Sirius Red stainings were performed as previously described to analyze collagen accumulation.[5] Stained tissue sections were viewed using a Zeiss Axio Imager M1 microscope, and digital images were acquired with an AxioCamICc3 camera (Zeiss) and processed using Fiji software. Positive staining was calculated as the percentage of the stained area, dividing the positive area by the whole area of the tissue analyzed.

Statistical analysis

In the in vitro studies, FAPs and satellite cells isolated from mice were used as experimental units. Cells treated with the HDACi and cells treated with the solvent (controls) were compared. In the in vivo experiments, the supraspinatus and infraspinatus muscles isolated from each mouse were considered as the experimental units. Comparisons were made between muscles from healthy and RC-injured mice, as well as between those from injured mice exposed to vorinostat or its solvent. Additionally, muscles from healthy mice were compared to those from injured mice either exposed or not exposed to vorinostat. Sample size was calculated using the G*Power programme, with the effect size (f) calculated after fixing the significance level ($\alpha = 0.05$) and the statistical power ($1\text{-}\beta = 90\%$). All statistical analyses were performed using SPSS 15.0 (SPSS, USA). The Shapiro-Wilk test was used to assess normal distribution. Variables were analyzed with the Mann-Whitney U test or independent-samples *t*-test. All experiments were performed using at least three independent experiments per each condition. Data are expressed as mean and standard error of the mean (SEM). Any p-values < 0.05 were considered to be statistically significant.

Results

HDAC inhibitors abrogate the adipogenic potential of FAPs

FAPs were treated with three different HDACis, including entinostat, vorinostat, and quisinostat, for six consecutive days, finding a notable decrease in the adipogenic transformation of FAPs compared to control cells. Specifically, entinostat treatment led to a 55% (SEM 3.1%) reduction in perilipin expression levels, a hallmark for adipocytes, in FAPs at a concentration of 2 μM and a 14% (SEM 6.5%) reduction at a concentration of 4 μM (Figures 1a and 1d). The effect of vorinostat on FAPs was dose-dependent, with a 60% (SEM 3.3%), 70% (SEM 1.97%), and 87% (SEM 2.97%) reduction in perilipin expression at concentrations of 1 μM, 2 μM, and 4 μM, respectively (Figures 1b and 1e). On the other hand, quisinostat consistently reduced perilipin expression by 97% (SEM 0.3%) (Figures 1c and 1f), even at very low doses (10 nM, 20 nM, and 30 nM).

Vorinostat induces satellite cell-myogenic recruitment through its action on FAPs

Next, we assessed the potential impact of the epigenetic compounds to increase in vitro myogenic differentiation of the satellite cells by measuring the ability of the cells to fuse in myotubes. Quisinostat treatment was toxic to the satellite cells, while 2 μM entinostat resulted in a significant reduction in the expression of the myogenic differentiation marker myosin (MyHC) in satellite cells (Figure 2a to 2b), indicating a loss of myogenic recruitment. In contrast, 1 μM vorinostat did not affect the myogenic potential of the satellite cells (Figure 2c to 2d), which fused into myotubes as control cells. Interestingly, when FAPs were treated with 1 μM vorinostat and the conditioned media from these treated FAPs was added to the satellite cells (indirect treatment), there was a twofold increase in MyHC expression in the cells (Figure 2e to 2f), demonstrating a pro-myogenic effect.

Vorinostat blocks HDAC activity in FAPs but not in satellite cells

We next analyzed the epigenetic effect of vorinostat in FAPs and satellite cells by measuring the acetylation levels of histone 3 (H3Ac). The average intensity levels of H3Ac increased in FAPs after the addition of 1 μM vorinostat (Figure 3a to 3b). However, the same dose of vorinostat did not modify the histone acetylation status of the satellite cells, when added directly to the myogenic cells (Figure 3c to 3d) or indirectly through the conditioned media from treated FAPs (Figure 3e to 3f).

These results suggest that vorinostat can prevent FAPs from differentiating into adipocytes through its acetylation activity. This, in turn, indirectly promotes the fusion of satellite cells into myotubes through a non-histone acetylation mechanism.

Vorinostat protects muscles from acute degeneration after rotator cuff rupture

We next investigated vorinostat's potential to mitigate muscle degeneration after RC injury. Complete section of the supra- and infraspinatus tendons and section of the suprascapular nerve in wild-type mice induced an atrophic and degenerative muscle response. This was characterized by reduced muscle fibre CSA, higher hypercellular and centrally nucleated fibres, increased fibrosis, and fatty accumulation in both the inter- and intrafascicular space (Supplementary Figures da to de). These changes were evident from day 14 to 28 after tenotomy, preceded by an early increase of inflammatory cells, especially in the supraspinatus (Supplementary Figure df).

Subsequently, adult wild-type injured mice were exposed to vorinostat (5 mg/kg) for 12 consecutive days, starting two days after tenotomy. While full recovery of healthy muscle phenotypic features was not achieved, vorinostat resulted in notable improvements compared to injured mice that received a control treatment (Figure 4). Vorinostat reduced cellular inflammation, especially in the infraspinatus, and intramuscular fatty infiltration, particularly noticeable in the supraspinatus (Figure 4a to 4c). However, fibrosis accumulation persisted despite vorinostat exposure (Figure 4d to 4e). In addition, vorinostat attenuated the muscular atrophy response, evidenced by increased fibre CSA and a reduction in the number of smaller fibres compared

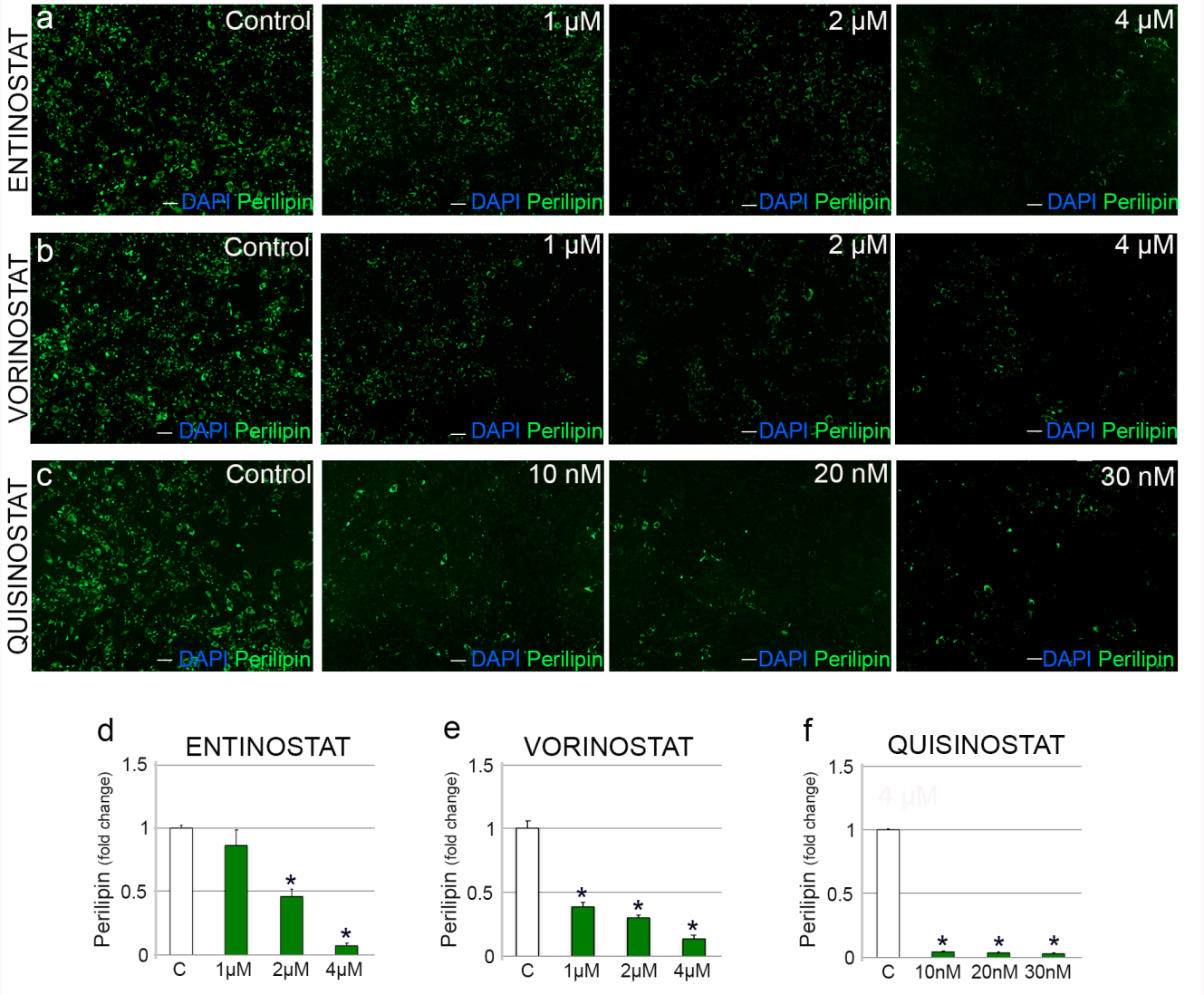

Fig. 1

Histone deacetylase inhibitors (HDACis) decrease the adipogenic potential of fibro-adipogenic progenitors (FAPs). Representative images of FAPs immunostained for perilipin after the daily administration of a) entinostat, b) vorinostat, or c) quisinostat. 4',6-diamidino-2-phenylindole (DAPI) was used to identify all nuclei. Scale bar: 10 μm. d) to f) Graphs show the quantification of perilipin in FAPs, considering control untreated cells as 1. Numerical data in HDACi-treated cells were expressed as a fold change compared to control cells. Data were expressed as the mean and standard error of the mean of at least three independent experiments. *Significance between control and experimental groups where $p < 0.05$, Shapiro Wilk and Mann-Whitney U tests.

to healthy and control-treated injured mice (Figure 4f to 4h, Supplementary Figure e), particularly pronounced in the infraspinatus muscles. Importantly, differences in the repair response of the infra- and supraspinatus muscles were not linked to fibre types, with both muscles exhibiting a similar composition, predominantly comprising type IIB and type IIX fibres, and a lesser contribution from type IIA fibres (Supplementary Figure ec and ed).

Vorinostat decreases the numbers of fibro-adipogenic progenitors in muscles after acute rotator cuff rupture

Tenotomy increased the numbers of FAPs and satellite cells (Figure 5a to 5e) in both supra- and infraspinatus muscles. Vorinostat decreased the abundance of FAPs (Figure 5a to 5b), particularly in the supraspinatus muscles. Although tenotomy increased the number of muscle stem cells, vorinostat did not alter the overall count of $Pax7^+$ satellite cells. The numbers of $Pax7^+Ki67^-$ quiescent and $Pax7^+Ki67^+$ proliferating satellite cells were comparable between the treated and control injured mice (Figure 5c to 5e). However, examining the phenotypic distribution of satellite cells revealed a significant increase in the percentage of proliferating satellite cells over quiescent satellite cells in the supraspinatus muscles treated with vorinostat, compared to control-treated injured mice (Figure 5f). This suggests that vorinostat promotes a more favourable response to muscle injury.

Vorinostat partially increases H3Ac status in the muscle two weeks after RC

Tenotomy increased the H3Ac status of muscles, notably in the supraspinatus muscles (Figure 6a to 6b), compared to healthy mice. One notable finding was that vorinostat significantly increased infraspinatus H3Ac levels (Figure 6a to 6b), which may be attributed to the elevated expression levels of H3Ac

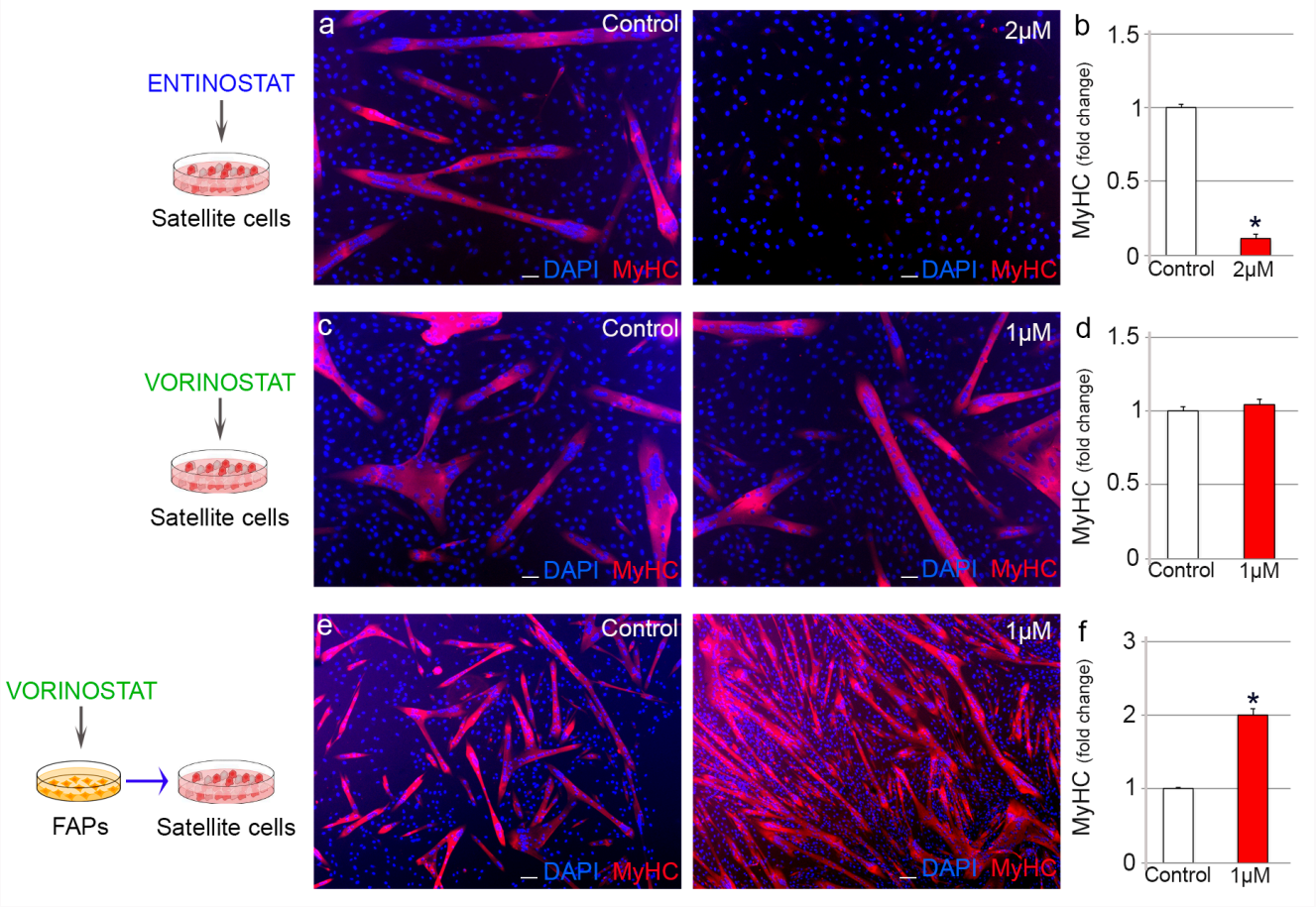

Fig. 2

Vorinostat modifies the myogenic potential of satellite cells through its effect on fibro-adipogenic progenitors (FAPs). a), c), and e) Representative images of satellite cells immunostained for myosin (MyHC), and b), d), and f) quantification of the myogenic differentiation after the a) to d) direct or e) and f) indirect daily administration of histone deacetylase inhibitor (HDACi). 4',6-diamidino-2-phenylindole (DAPI) was used to identify all nuclei. Scale bar, 10 μm. Numerical data in HDACi-treated cells were expressed as a fold change compared to control cells, and expressed as the mean and standard error of the mean of at least three independent experiments. *Significance between experimental groups where $p < 0.05$.

in FAPs (Figure 6c to 6d). Although the histone acetylation status of Pax7$^+$ satellite cells tended to increase after injury, particularly in proliferating muscle stem cells, there were no differences between vorinostat-treated and control injured muscles (Figure 6e to 6h). Thus, vorinostat could hinder early muscle fatty degeneration by exerting its effects on FAPs, especially in the injured infraspinatus muscles.

Vorinostat fails to prevent muscle degeneration in the chronic phase of RC damage

We extended the exposure to vorinostat for an additional 14 days, finding that its impact on muscle atrophy and degeneration was not evident during the chronic phase following RC injury. At 28 days, comparable levels of muscular inflammation, fatty infiltration, fibrosis, and atrophy were observed between vorinostat-treated and control-treated injured mice (Figure 7a to 7g), all of which were upregulated compared to healthy mice. Moreover, the differences observed between vorinostat-treated and control-treated injured mice at 14 days after RC injury were no longer apparent at 28 days (Figure 7a to 7g).

At 28 days post-tenotomy, no notable differences were found in the number of FAPs and satellite cells between vorinostat-treated and non-treated injured mice (Supplementary Figure f). PDGFRα$^+$ cell numbers remained higher at day 28 after tenotomy compared to healthy mice, while satellite cell numbers tended to return to basal values (Supplementary Figures fa to fd). Furthermore, muscle H3Ac levels and the accumulation of H3Ac in FAPs and satellite cells were similar between muscles from injured and healthy mice, reaching comparable levels (Supplementary Figures fe to fi).

These results show that vorinostat's potential to inhibit the adipogenic transformation of FAPs, promote myogenic recruitment, and protect muscles from acute degeneration is lost in the chronic phase after RC injury.

Vorinostat increases angiogenesis after RC in the injury chronic phase

We next analyzed the angiogenesis process following tenotomy. Two weeks after injury, there were no significant differences in the presence of small (CD31) and large (CD31/αSMA) vessels between muscles from healthy and injured mice, and vorinostat did not induce an angiogenic response (Figure 8). However, CD31$^+$ endothelial cells accumulated in both supraspinatus and infraspinatus muscles of injured mice after extended drug exposure (Figure 8a to 8b). Likewise, vorinostat promoted the formation of large vessels in muscles 28 days after injury (Figures 8a and 8c).

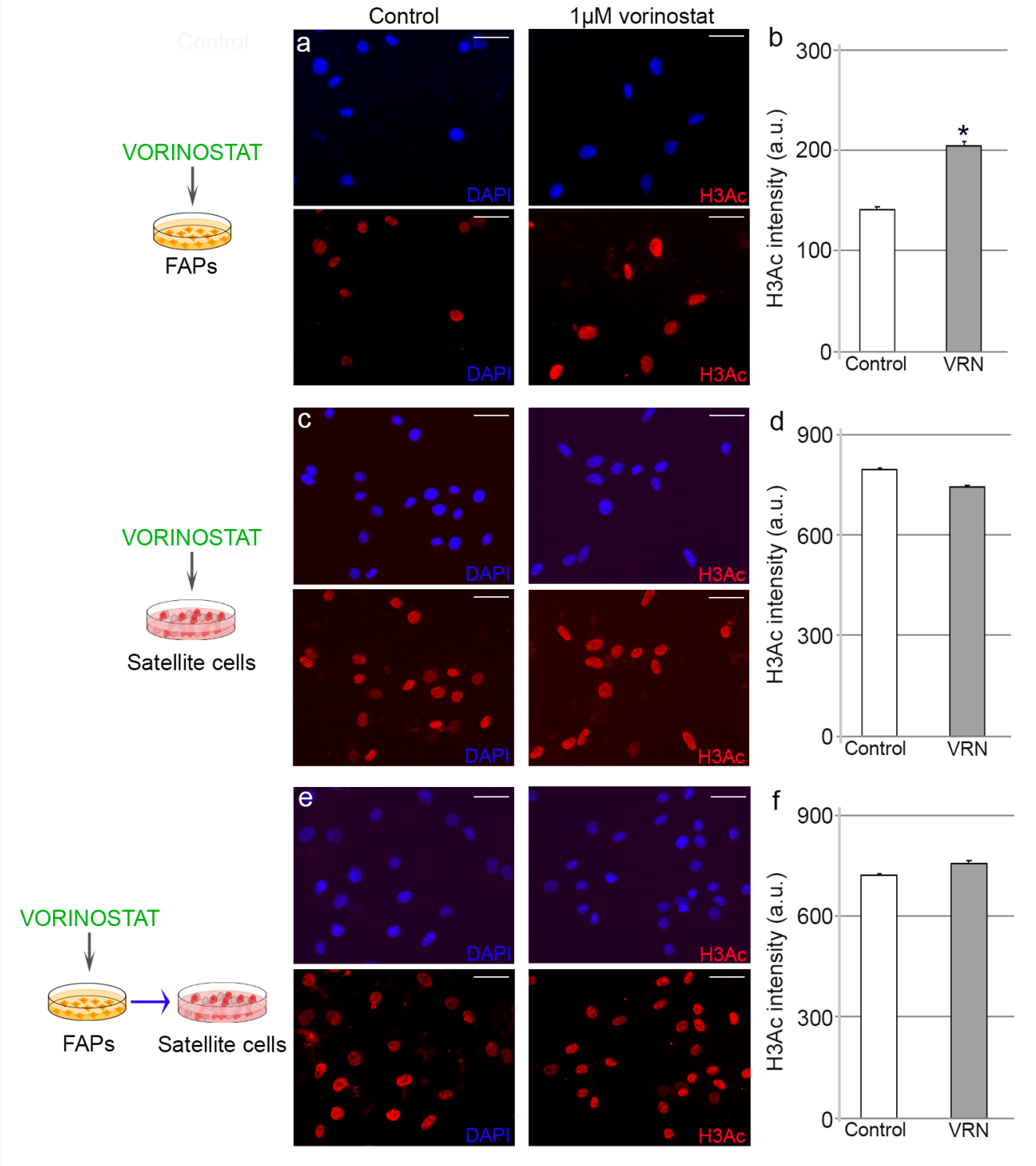

Fig. 3

Vorinostat modifies histone acetylation levels in fibro-adipogenic progenitors (FAPs). Representative images of a) FAPs and c) and e) satellite cells from control and vorinostat-treated groups immunostained for histone 3 acetylation (H3Ac) after the a) and c) direct or e) indirect addition of the histone deacetylase inhibitor. Graphs in b), d), and f) show the mean H3Ac intensity accumulated in the cells. 4',6-diamidino-2-phenylindole (DAPI) was used to identify all nuclei. Scale bar, 10 µm. Numerical data were expressed as the mean and standard error of the mean of at least three independent experiments. *Significance between experimental groups where $p < 0.05$, Shapiro Wilk and Mann-Whitney U tests. a.u., arbitrary units; VRN, vorinostat.

Discussion

Our findings suggest that HDACi vorinostat has potential implications for the modulation of muscle degeneration and regeneration after RC injury. It effectively reduces the in vitro adipogenic potential of FAPs by increasing their histone acetylation status, which indirectly promotes the recruitment of satellite cells towards myogenic differentiation. Regarding the in vivo experiments, vorinostat led to improvements in muscle phenotypic features compared to the control-injured group, reducing cellular inflammation and intramuscular fatty

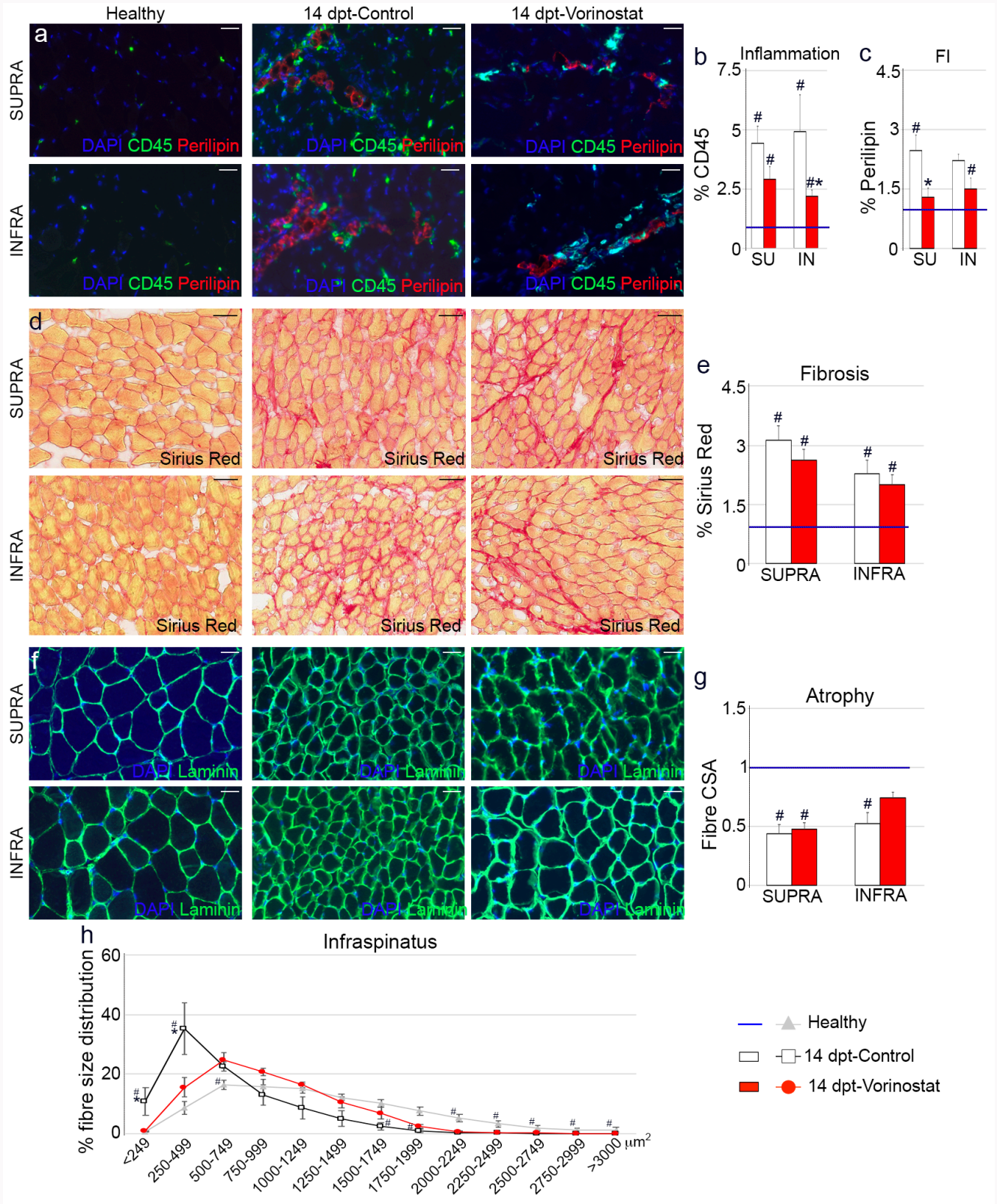

Fig. 4

Vorinostat reduces muscle degeneration after tenotomy. Representative images of immunostained muscle tissue sections for a) CD45/Perilipin, d) Sirius red, and f) laminin from healthy (n = 6) and injured mice, treated (n = 4) or not treated (n = 4) with vorinostat for 12 days, two days after rotator cuff (RC) injury. 4',6-diamidino-2-phenylindole (DAPI) was used to identify all nuclei. Scale bar, 10 µm. Graphs show the presence of b) cellular, c) fatty, and e) fibrotic accumulation in the muscles. g) Mean cross-sectional area of the supra- and infraspinatus muscles from healthy and vorinostat-treated and untreated injured mice. h) Fibre size distribution of the infraspinatus muscles from the different experimental conditions. Data were expressed as the mean and standard error of the mean, where expression levels were related to those found in healthy muscles, which were considered as 1 (blue line). *Significance between control and vorinostat-treated injured mice. '#' defines significance between healthy and injured mice, where $p < 0.05$, Shapiro-Wilk test, Mann-Whitney U test, and independent-samples *t*-test. dpt, days post-tenotomy; FI, fatty infiltration; IN and INFRA, infraspinatus; SU and SUPRA, supraspinatus.

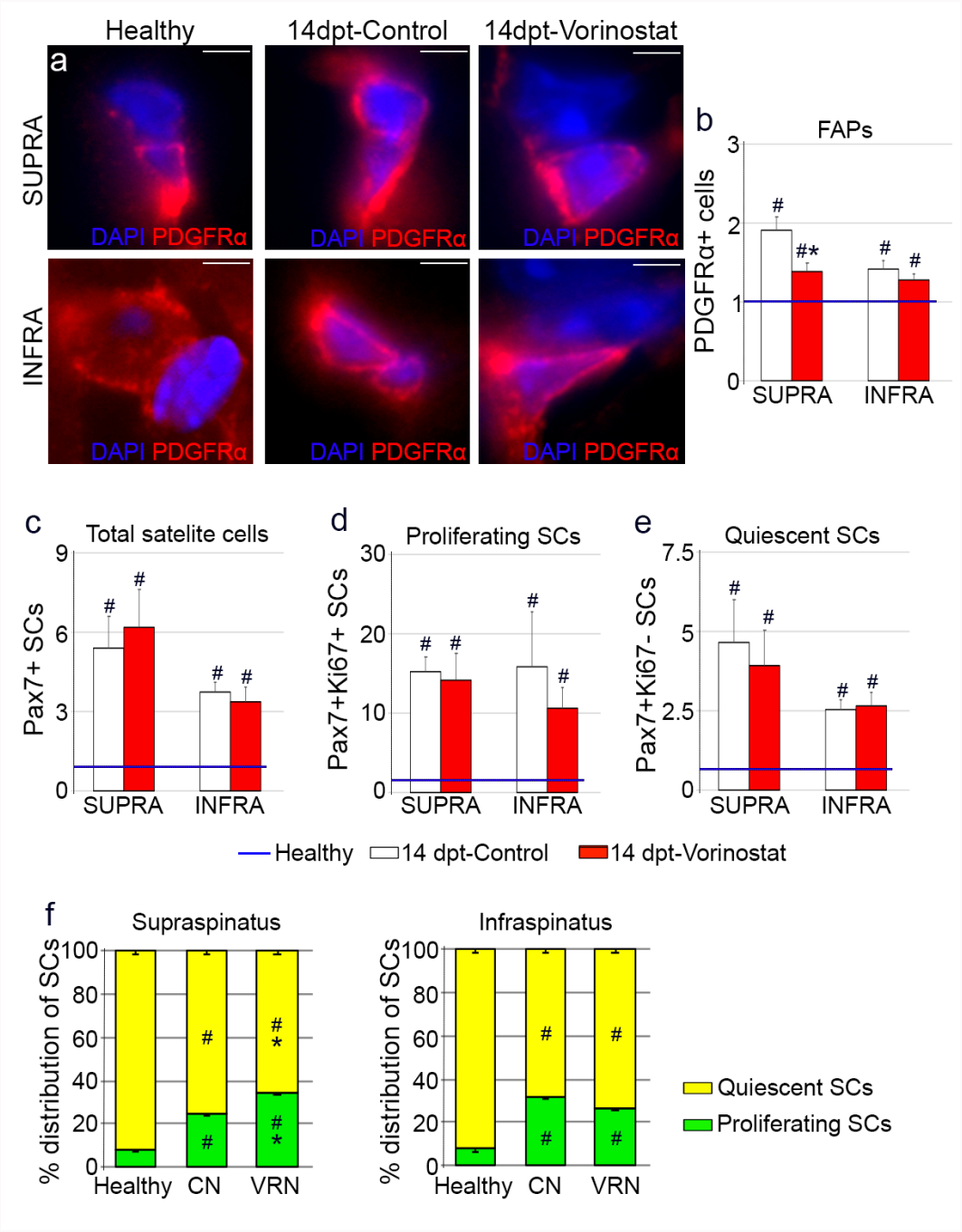

Fig. 5

Vorinostat-treated mice reduce the accumulation of fibro-adipogenic progenitor cells (FAPs) after tenotomy. Representative images of muscles from healthy and injured mice, treated or not treated with vorinostat, immunostained for a) PDGFRα to b) quantify the presence of FAPs. 4',6-diamidino-2-phenylindole (DAPI) was used to identify all nuclei. Scale bar, 40 μm. Graphs show the presence of c) total Pax7+, d) proliferating Pax7+ Ki67+, and e) quiescent Pax7+ Ki67-satellite cells in the supra- and infraspinatus muscles under healthy and injured conditions. Graphs in f) show the percentage of distribution of total satellite cells (SCs) considering their cellular status. Measurements were expressed as the mean and standard error of the mean of at least four biological replicates per condition, and expressed as the fold change considering healthy muscles as 1 (blue line). *Significance between control- and vorinostat-treated injured mice. '#' identifies significance between healthy and injured mice, where $p < 0.05$, Shapiro Wilk test, Mann-Whitney U test, and independent-samples *t*-test. CN, control; dpt, days post-tenotomy; INFRA, infraspinatus; SUPRA, supraspinatus; VRN, vorinostat.

infiltration, and attenuating muscular atrophy. These findings seem to be beneficial for RC repair and highlight a positive effect of vorinostat in the FAP-satellite cell relationship, since FAPs contribute to adipose tissue infiltration and muscle degeneration, while satellite cells are essential for muscle repair.[11,18] However, vorinostat did not prevent the accumulation of fibrosis caused by tenotomy. Furthermore, it did not demonstrate a significant effect on muscle degeneration in an advanced phase of RC damage, suggesting that its beneficial effect may weaken over time.

There are some intriguing results in our study that should be acknowledged for future research: for example, the differential behaviour found between the supra- and infraspinatus muscles after the short-term treatment

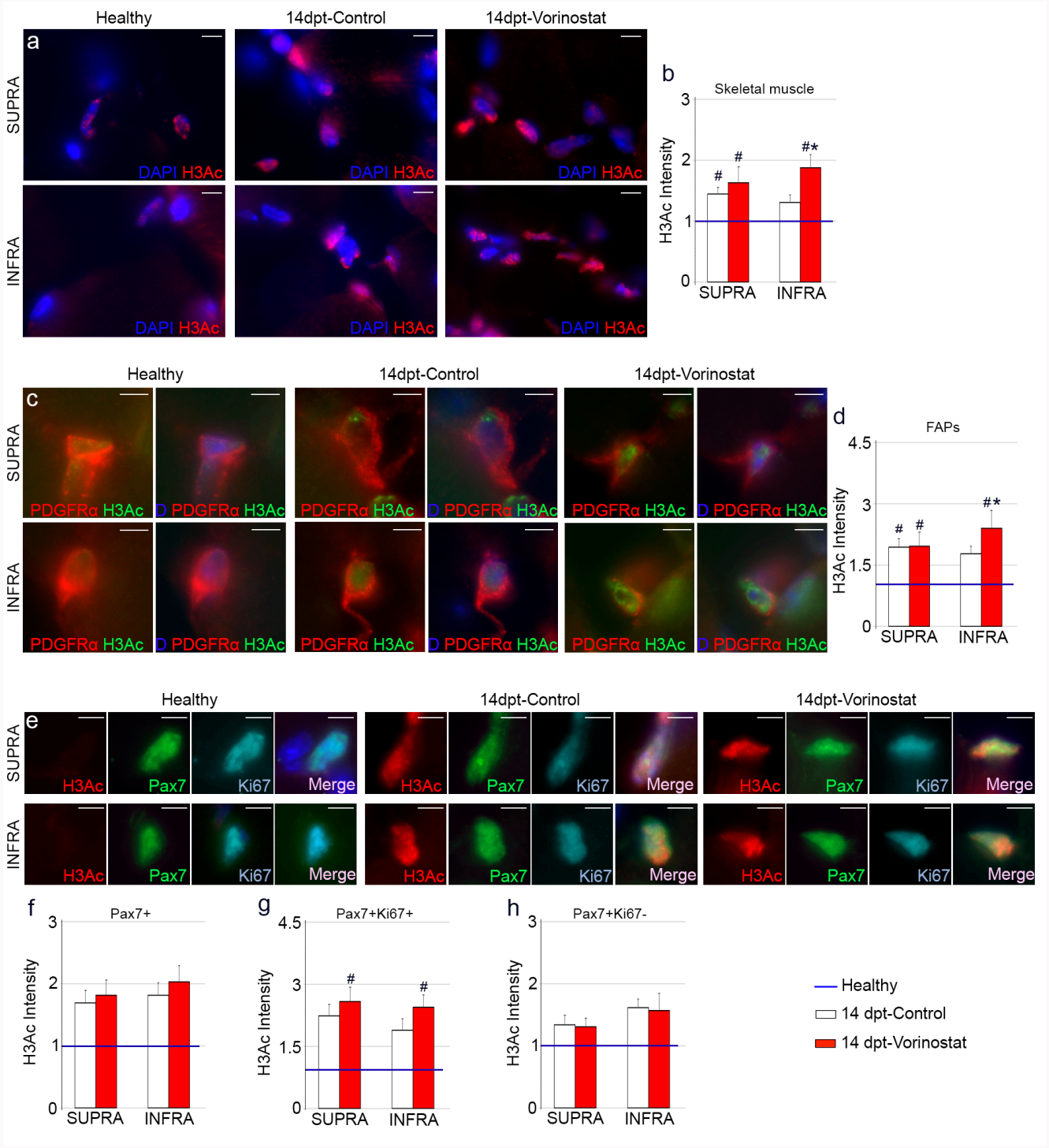

Fig. 6

Vorinostat induces the expression of histone 3 acetylation (H3Ac) in the infraspinatus muscles and their fibro-adipogenic progenitors (FAPs) after tenotomy. Supra- and infraspinatus muscles from healthy and control/vorinostat-treated injured mice immunostained for a) H3Ac, c) H3Ac/PDGFRα, and e) H3Ac/Pax7/Ki67. 4',6-diamidino-2-phenylindole (DAPI) was used to identify all nuclei. Scale bar, 40 μm. Graphs show the accumulation of H3Ac in b) the muscle, d) FAPs, and f) to h) Pax7+ satellite cells (SCs). Data were expressed as the mean and standard error of the mean of at least four biological replicates per condition, where expression levels were related to those found in healthy muscles, which were considered as 1 (blue line). *Significance between control and vorinostat-treated injured mice. '#' identifies significance between healthy and injured mice, where $p < 0.05$, Shapiro-Wilk test, Mann-Whitney U test, and independent-samples *t*-test. dpt, days post-tenotomy; INFRA, infraspinatus; SUPRA, supraspinatus.

with vorinostat in tenotomy-injured mice, which suggests potential cell-specific differences in the response to the HDACi vorinostat treatment. This would be a key factor in a tissue like the skeletal muscle, which is composed of heterogeneous cell subpopulations, such as FAPs and satellite cells,[19] that interact with each other[11,20] and with other muscle-resident and infiltrating cell subpopulations,[21] such as inflammatory cells,[22,23] after injury. Heterogeneity of muscle-associated cells depends on anatomical localization, tissue functionality, and severity of pathological situation.[23-25]

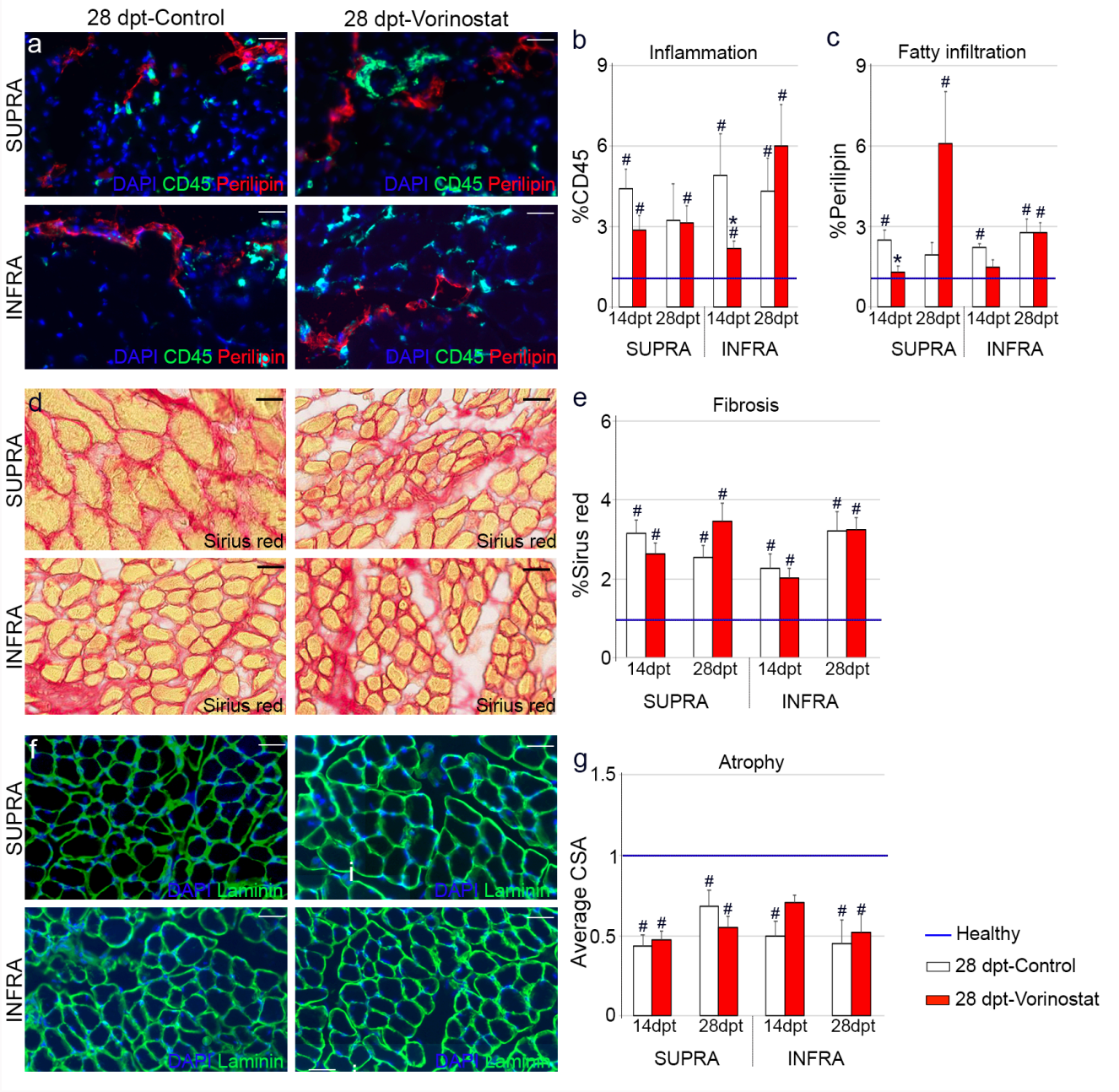

Fig. 7

The beneficial effect of vorinostat in tenotomy-induced muscles is lost in the chronic disease stage. Representative images of supra- and infraspinatus muscles from rotator cuff-injured mice, which received or did not receive vorinostat treatment, immunostained for a) CD45/Perilipin, d) Sirius red, and f) laminin. 4',6-diamidino-2-phenylindole (DAPI) was used to identify all nuclei. Scale bar, 40 μm. Graphs show b) inflammation, c) fatty infiltration, e) fibrosis, and g) atrophy. Data were expressed as the mean and standard error of the mean of at least four biological replicates per condition, related to levels found in healthy muscle (blue line) and expressed as a fold change. *Significance between control and vorinostat-treated injured mice. '#' identifies significance between healthy and injured mice, where $p < 0.05$, Shapiro-Wilk test, Mann-Whitney U test, and independent-samples *t*-test. CSA, cross-sectional area; dpt, days post-tenotomy; INFRA, infraspinatus; SUPRA, supraspinatus.

The infraspinatus and supraspinatus muscles have different functions on the glenohumeral joint in the shoulder that may potentially influence their regenerative capacities.[26] Muscle function determines muscle fibre type composition, impacting satellite cell response.[27] As FAPs actively participate in muscle homeostasis and repair, their behaviour may also be influenced by the specific microenvironment created by different muscle fibres. Nevertheless, our findings show that both the supraspinatus and infraspinatus muscles share a similar structural composition. FAP-specific activation state may also affect cell behaviour response to vorinostat, and our study shows that the supraspinatus and infraspinatus muscles were not equally affected by the injury procedure, as previously demonstrated by others.[28] Moreover, injury disease stage may further explain why the benefits of vorinostat treatment after RC injury decrease over time. Preclinical studies in muscular disorders indicate that the beneficial effects of the pan-HDACi trichostatin A are restricted to early stages of disease.[14,29] This has been associated with FAPs exhibiting aberrant HDAC activity with genome-wide

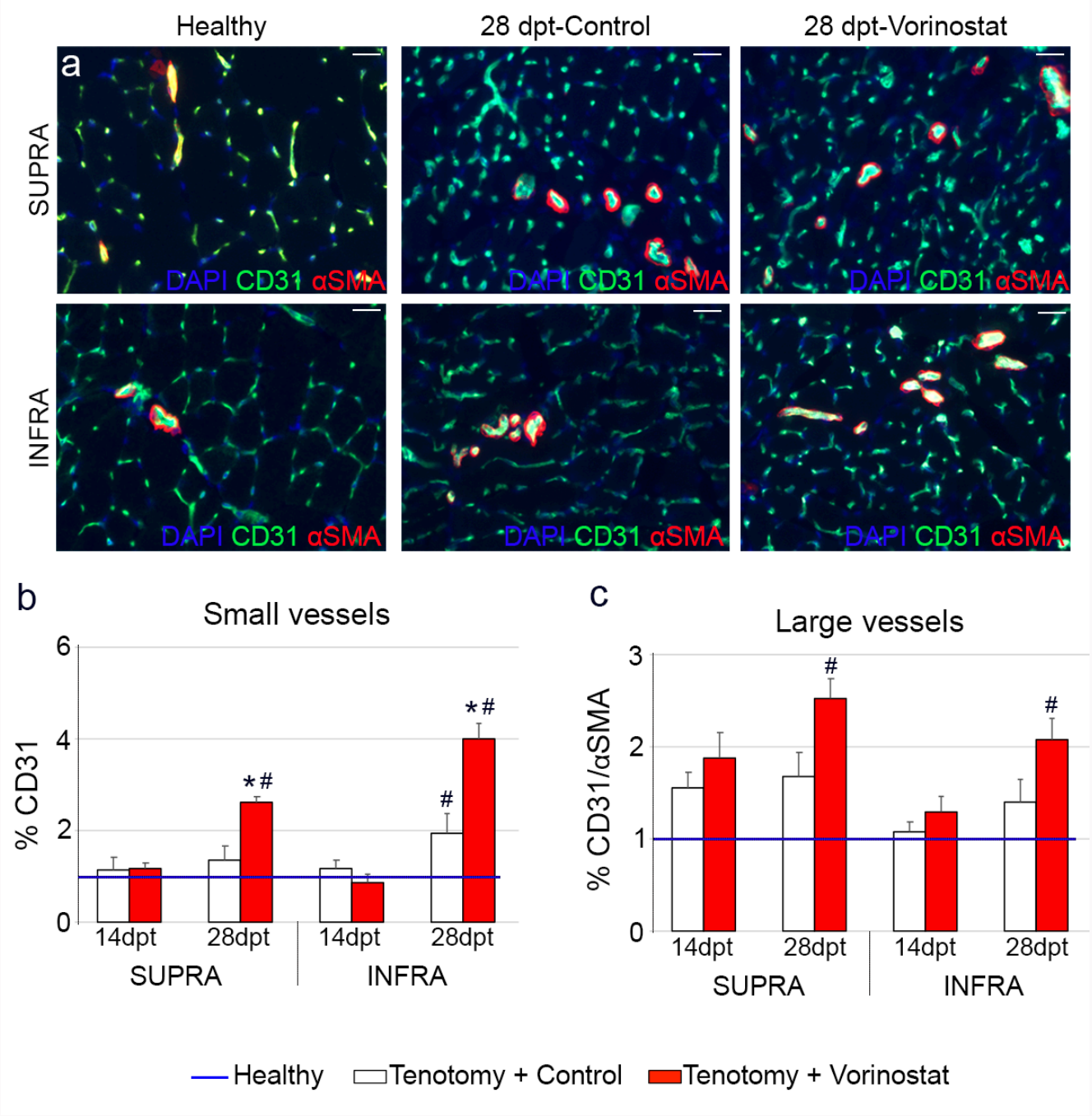

Fig. 8

Vorinostat induces the presence of small and large vessels in the muscles from injured mice 28 days after tenotomy. a) Representative images of the supra- and infraspinatus muscles from healthy and vorinostat treated/untreated-injured mice immunostained for CD31/αSMA. 4',6-diamidino-2-phenylindole (DAPI) was used to identify all nuclei. Scale bar, 40 μm. Graphs show the presence of b) small and c) large vessels in the infra- and supraspinatus muscles. Data were expressed as the mean and standard error of the mean of at least four biological replicates per condition, where expression levels were related to those found in healthy muscles, which were considered as 1 (blue line). *Significance between control and vorinostat-treated injured mice. '#' identifies significance between healthy and injured mice, where $p < 0.05$, Shapiro-Wilk test and independent-samples *t*-test. dpt, days post-tenotomy; INFRA, infraspinatus; SUPRA, supraspinatus.

alterations of acetylation, and with a senescent state of FAPs that are not fully reversed by the epigenetic molecules.[30] Thus, functional heterogeneity between FAPs from the supra- and infraspinatus muscles, associated with injury stage, may influence the mechanisms through which vorinostat modulates tissue repair, and consequently modify the FAP-satellite cell relationship. This indicates the importance of a permissive environment within regenerating muscles for the beneficial action of vorinostat, suggesting that our RC injury model develops a disease-associated resistance in the late stages of injury that might limit the efficacy of the treatment. Accordingly, the action of HDACi may vary based on cell type and experimental conditions, impacting differently gene expression patterns, growth factors, cell proliferation, and remodelling processes. To what extent the heterogeneity response to vorinostat after RC injury reflects different anatomical location

of different FAP subtypes/states, and their interaction with the satellite cells and other muscle-associated cells, remains to be investigated. Additionally, whether the presence of senescent FAPs after RC injury influences vorinostat effectiveness is a new open therapeutic opportunity for future investigation.

Given the elevated levels of H3Ac observed in FAPs, proliferating satellite cells, and muscles within the early stage of RC-injured mice, one might expect an increase of histone acetylation during muscle repair. However, the reality is quite the opposite, and histone acetylation is globally diminished during myogenesis,[31] according to higher HDAC activity after RC injury,[32] circumstances that are closer to our advanced RC injury stage. The same can be said of the unexpectedly low increase in the levels of H3Ac observed in FAPs and satellite cells exposed to vorinostat contrast, with its anticipated effect in promoting histone hyperacetylation. This paradoxical phenomenon can likely be attributed to the multifaceted impact of vorinostat on various histone acetylation-dependent and independent processes, as suggested before for other HDACis.[33,34] Furthermore, HDACis can exert their influence on histone and non-histone proteins, leading to changes in gene expression patterns and cellular responses. For example, the transcription factors Mef2 and MyoD are acetylated during myogenic differentiation, and their acetylation promotes myogenesis,[35] while non-histone acetylation increases have been detected in specific gene promoters in FAPs.[30] Moreover, the overall outcome of subjecting FAPs and satellite cells to systemic vorinostat exposure may hinge on a complex interplay of direct and indirect effects, with signals originating from other muscle-resident cell types concurrently exposed to vorinostat.[36] According to this idea, vorinostat has the capacity to act on inflammatory cells, reducing the production of proinflammatory cytokines,[37] which modulate FAP-satellite cell interaction in an injury stage-dependent manner.[11,22] Moreover, although HDACis can cause anti-angiogenic effects under tumorigenic conditions, they have pro-angiogenic effects in particular tissue remodelling processes.[38] In agreement with this latter statement, vorinostat increased angiogenesis in late-stage RC injury, when new blood vessel formation is required for tissue repair. Unfortunately, the exact mechanisms through which HDACis modulate angiogenesis are not fully understood, and less is known regarding the role of the angiogenic process during RC injury progression.

It is important to acknowledge certain considerations that can be regarded as limitations of our study. Contralateral supraspinatus and infraspinatus muscles after sham surgery were not used as healthy controls in our study, as contralateral muscles are often affected asymptomatically in unilateral RC injury, and sham surgeries may induce an inflammatory response that would influence the muscles under study.[39] Although spontaneous healing of supraspinatus and infraspinatus tendons after transection can occur, it does not prevent muscle degeneration occurring after RC injury.[28,40] Notably, our study did not include long-term stages of RC injury, during which muscular fatty infiltration becomes more prominent. Our research was focused on the hypothesis that vorinostat plays a role in early-to-middle stage of RC injury, when there is observable evidence of degenerative changes in the supraspinatus and infraspinatus muscles, which are preceded by an inflammatory peak response. This specific timeframe enables the investigation of the initial interactions between FAPs and satellite cells following injury initiation, an interaction primarily triggered by inflammatory cells.[11,22] Denervation is a rare event associated with clinical RC injury, but it ensures rapid muscular atrophy and fat tissue accumulation after tendon resection,[32] allowing the study of early FAP-satellite cell interaction under vorinostat exposure, which was the aim of our work.

At the time of writing, there are 854 clinical trials in the USA employing HDACis, predominantly focusing on their beneficial effects in cancer-related diseases.[41] Vorinostat, in particular, is being used in 276 studies. These findings, coupled with vorinostat's overall positive effects in the acute phase following tenotomy, may prompt orthopaedics to consider its application in clinical trials for RC tears, especially in cases where the degree of muscle degeneration influences the decision to repair the ruptured tendon.[42] In these situations, employing an animal model that replicates the disease and repair process, mirroring scenarios encountered in clinical practice, could offer valuable insights into the effectiveness of short-term vorinostat treatment. This might involve mimicking the delayed repair often seen in clinical practice, considering the muscle condition with vorinostat both at the time of surgery and after surgery. However, caution is essential. Thoroughly uncovering the potential side effects of vorinostat is crucial to ensuring its safety as a therapeutic strategy, while understanding why its beneficial effects are lost in the chronic disease phase after tenotomy is essential for a comprehensive evaluation. Exploring alternative dosing patterns, such as pulse dosing and/or localized and controlled release, could prove beneficial for both short- and long-term treatments. This will not only offer a more feasible application in humans, but also has the potential to reduce the required effective dose and thus minimize potential risks.

Our study serves as a starting point to introduce a range of new approaches for using and validating vorinostat in studies with a more clinical focus, thereby bridging the gap between basic research and therapeutic strategies. Our findings suggest that the HDACi vorinostat has the potential to therapeutically counteract muscle degeneration in the early stages of RC injury. The stage-specific response of FAPs to vorinostat encourages further research to elucidate its mechanisms of action and identify more selective strategies to halt the progression of RC injury. Additional studies are needed to fully comprehend vorinostat's effects on cell-to-cell interactions and cellular processes for muscle restoration after RC injury, thereby optimizing its therapeutic benefits in long-term damage stages.

Supplementary material

Figures designed to elucidate the material and methods employed in the study, as well as to provide additional information complementing the study results. An ARRIVE checklist is also included to show that the ARRIVE guidelines were adhered to in this study.

References

1. **Yamamoto A**, **Takagishi K**, **Osawa T**, **et al**. Prevalence and risk factors of a rotator cuff tear in the general population. *J Shoulder Elbow Surg*. 2010;19(1):116–120.
2. **Valencia AP**, **Lai JK**, **Iyer SR**, **et al**. Fatty infiltration is a prognostic marker of muscle function after rotator cuff tear. *Am J Sports Med*. 2018;46(9):2161–2169.
3. **Liu X**, **Ning AY**, **Chang NC**, **et al**. Investigating the cellular origin of rotator cuff muscle fatty infiltration and fibrosis after injury. *Muscles Ligaments Tendons J*. 2016;6(1):6–15.
4. **Uezumi A**, **Fukada S**, **Yamamoto N**, **Takeda S**, **Tsuchida K**. Mesenchymal progenitors distinct from satellite cells contribute to ectopic fat cell formation in skeletal muscle. *Nat Cell Biol*. 2010;12(2):143–152.
5. **Jensen AR**, **Kelley BV**, **Mosich GM**, **et al**. Neer Award 2018: Platelet-derived growth factor receptor α co-expression typifies a subset of platelet-derived growth factor receptor β-positive progenitor cells that contribute to fatty degeneration and fibrosis of the murine rotator cuff. *J Shoulder Elbow Surg*. 2018;27(7):1149–1161.
6. **Chargé SBP**, **Rudnicki MA**. Cellular and molecular regulation of muscle regeneration. *Physiol Rev*. 2004;84(1):209–238.
7. **Mauro A**. Satellite cell of skeletal muscle fibers. *J Biophys Biochem Cytol*. 1961;9(2):493–495.
8. **Hsu W-B**, **Lin S-J**, **Hung J-S**, **et al**. Effect of resistance training on satellite cells in old mice - a transcriptome study: implications for sarcopenia. *Bone Joint Res*. 2022;11(2):121–133.
9. **Joe AWB**, **Yi L**, **Natarajan A**, **et al**. Muscle injury activates resident fibro/adipogenic progenitors that facilitate myogenesis. *Nat Cell Biol*. 2010;12(2):153–163.
10. **Heredia JE**, **Mukundan L**, **Chen FM**, **et al**. Type 2 innate signals stimulate fibro/adipogenic progenitors to facilitate muscle regeneration. *Cell*. 2013;153(2):376–388.
11. **Biferali B**, **Proietti D**, **Mozzetta C**, **Madaro L**. Fibro-adipogenic progenitors cross-talk in skeletal muscle: the social network. *Front Physiol*. 2019;10:1074.
12. **Wosczyna MN**, **Konishi CT**, **Perez Carbajal EE**, **et al**. Mesenchymal stromal cells are required for regeneration and homeostatic maintenance of skeletal muscle. *Cell Rep*. 2019;27(7):2029–2035.
13. **Shirasawa H**, **Matsumura N**, **Shimoda M**, **et al**. Inhibition of PDGFR signaling prevents muscular fatty infiltration after rotator cuff tear in mice. *Sci Rep*. 2017;7:41552.
14. **Mozzetta C**, **Consalvi S**, **Saccone V**, **et al**. Fibroadipogenic progenitors mediate the ability of HDAC inhibitors to promote regeneration in dystrophic muscles of young, but not old Mdx mice. *EMBO Mol Med*. 2013;5(4):626–639.
15. **Iezzi S**, **Di Padova M**, **Serra C**, **et al**. Deacetylase inhibitors increase muscle cell size by promoting myoblast recruitment and fusion through induction of follistatin. *Dev Cell*. 2004;6(5):673–684.
16. **Sandonà M**, **Cavioli G**, **Renzini A**, **et al**. Histone deacetylases: molecular mechanisms and therapeutic implications for muscular dystrophies. *Int J Mol Sci*. 2023;24(5):4306.
17. **Colussi C**, **Banfi C**, **Brioschi M**, **et al**. Proteomic profile of differentially expressed plasma proteins from dystrophic mice and following suberoylanilide hydroxamic acid treatment. *Proteomics Clin Appl*. 2010;4(1):71–83.
18. **Theret M**, **Rossi FMV**, **Contreras O**. Evolving roles of muscle-resident fibro-adipogenic progenitors in health, regeneration, neuromuscular disorders, and aging. *Front Physiol*. 2021;12:673404.
19. **Collins BC**, **Kardon G**. It takes all kinds: heterogeneity among satellite cells and fibro-adipogenic progenitors during skeletal muscle regeneration. *Development*. 2021;148(21):dev199861.
20. **Molina T**, **Fabre P**, **Dumont NA**. Fibro-adipogenic progenitors in skeletal muscle homeostasis, regeneration and diseases. *Open Biol*. 2021;11(12):210110.
21. **Johnson AL**, **Kamal M**, **Parise G**. The role of supporting cell populations in satellite cell mediated muscle repair. *Cells*. 2023;12(15):1968.
22. **Kang X**, **Yang M-Y**, **Shi Y-X**, **et al**. Interleukin-15 facilitates muscle regeneration through modulation of fibro/adipogenic progenitors. *Cell Commun Signal*. 2018;16(1):42.
23. **Contreras O**, **Cruz-Soca M**, **Theret M**, **et al**. Cross-talk between TGF-β and PDGFRα signaling pathways regulates the fate of stromal fibro-adipogenic progenitors. *J Cell Sci*. 2019;132(19):jcs232157.
24. **Madaro L**, **Passafaro M**, **Sala D**, **et al**. Denervation-activated STAT3-IL-6 signalling in fibro-adipogenic progenitors promotes myofibres atrophy and fibrosis. *Nat Cell Biol*. 2018;20(8):917–927.
25. **Lee C**, **Agha O**, **Liu M**, **et al**. Rotator cuff fibro-adipogenic progenitors demonstrate highest concentration, proliferative capacity, and adipogenic potential across muscle groups. *J Orthop Res*. 2020;38(5):1113–1121.
26. **Mochizuki T**, **Sugaya H**, **Uomizu M**, **et al**. Humeral insertion of the supraspinatus and infraspinatus. *J Bone Joint Surg Am*. 2008;90-A(5):962–969.
27. **Fry CS**, **Noehren B**, **Mula J**, **et al**. Fibre type-specific satellite cell response to aerobic training in sedentary adults. *J Physiol*. 2014;592(12):2625–2635.
28. **Wu G**, **Hu VJ**, **McClintick DJ**, **et al**. Lateral to medial fibro-adipogenic degeneration are greater in infraspinatus than supraspinatus following nerve and tendon injury of murine rotator cuff. *J Orthop Res*. 2021;39(1):184–195.
29. **Saccone V**, **Consalvi S**, **Giordani L**, **et al**. HDAC-regulated myomiRs control BAF60 variant exchange and direct the functional phenotype of fibro-adipogenic progenitors in dystrophic muscles. *Genes Dev*. 2014;28(8):841–857.
30. **Consalvi S**, **Tucciarone L**, **Macrì E**, **et al**. Determinants of epigenetic resistance to HDAC inhibitors in dystrophic fibro-adipogenic progenitors. *EMBO Rep*. 2022;23(6):e54721.
31. **Asp P**, **Blum R**, **Vethantham V**, **et al**. Genome-wide remodeling of the epigenetic landscape during myogenic differentiation. *Proc Natl Acad Sci U S A*. 2011;108(22):E149–58.
32. **Liu X**, **Liu M**, **Lee L**, **et al**. Trichostatin A regulates fibro/adipogenic progenitor adipogenesis epigenetically and reduces rotator cuff muscle fatty infiltration. *J Orthop Res*. 2021;39(7):1452–1462.
33. **Sanchez GJ**, **Richmond PA**, **Bunker EN**, **et al**. Genome-wide dose-dependent inhibition of histone deacetylases studies reveal their roles in enhancer remodeling and suppression of oncogenic super-enhancers. *Nucleic Acids Res*. 2018;46(4):1756–1776.
34. **Vaid R**, **Wen J**, **Mannervik M**. Release of promoter-proximal paused Pol II in response to histone deacetylase inhibition. *Nucleic Acids Res*. 2020;48(9):4877–4890.
35. **Sincennes MC**, **Brun CE**, **Rudnicki MA**. Concise review: epigenetic regulation of myogenesis in health and disease. *Stem Cells Transl Med*. 2016;5(3):282–290.
36. **Latroche C**, **Weiss-Gayet M**, **Muller L**, **et al**. Coupling between myogenesis and angiogenesis during skeletal muscle regeneration is stimulated by restorative macrophages. *Stem Cell Reports*. 2017;9(6):2018–2033.
37. **Richon VM**, **Zhou X**, **Rifkind RA**, **Marks PA**. Histone deacetylase inhibitors: development of suberoylanilide hydroxamic acid (SAHA) for the treatment of cancers. *Blood Cells Mol Dis*. 2001;27(1):260–264.
38. **Shen Z**, **Bei Y**, **Lin H**, **et al**. The role of class IIa histone deacetylases in regulating endothelial function. *Front Physiol*. 2023;14:1091794.
39. **Liu X**, **Joshi SK**, **Ravishankar B**, **Laron D**, **Kim HT**, **Feeley BT**. Upregulation of transforming growth factor-β signaling in a rat model of rotator cuff tears. *J Shoulder Elbow Surg*. 2014;23(11):1709–1716.
40. **Liu X**, **Laron D**, **Natsuhara K**, **Manzano G**, **Kim HT**, **Feeley BT**. A mouse model of massive rotator cuff tears. *J Bone Joint Surg Am*. 2012;94-A(7):e41.
41. **No authors listed**. ClinicalTrials.gov. https://clinicaltrials.gov/search?intr=HDAC (date last accessed 21 February 2024).
42. **Longo UG**, **Carnevale A**, **Piergentili I**, **et al**. Retear rates after rotator cuff surgery: a systematic review and meta-analysis. *BMC Musculoskelet Disord*. 2021;22(1):749.

Author information

L. Gil-Melgosa, PhD, Orthopaedic Surgeon
R. Llombart-Blanco, PhD, Orthopaedic Surgeon
J. Pons-Villanueva, PhD, Orthopaedic Surgeon
Orthopedic Surgery Department of Clínica Universidad de Navarra (CUN) and Instituto de Investigación Sanitaria de Navarra (IdiSNA), Pamplona, Spain.

L. Extramiana, Technician
G. Abizanda, BA, Veterinarian
A. Pérez-Ruiz, PhD, Researcher
Technological Innovation Division, Foundation for Applied Medical Research (FIMA), University of Navarra (UNAV) and IdiSNA, Pamplona, Spain.

I. Lacave, BA, Technician, Clinica Universidad de Navarra, Pamplona, Spain.

E. Miranda, BA, Technician
X. Agirre, PhD, Researcher
Hemato-Oncology Program, FIMA-UNAV and IdiSNA, Pamplona, Spain.

F. Prósper, PhD, Researcher, Hemato-Oncology Program, FIMA-UNAV and IdiSNA, Pamplona, Spain; Haematology Department, Clinica Universidad de Navarra, Pamplona, Spain; Centro de Investigación Biomédica en Red en Bioingeniería, Biomateriales y Nanomedicina (CIBER-BBN), Madrid, Spain.

A. Pineda-Lucena, PhD, Researcher, Medicinal Chemistry Program, FIMA-UNAV and IdiSNA, Pamplona, Spain.

Author contributions

L. Gil-Melgosara: Investigation, Writing – original draft, Writing – review & editing.
R. Llombart-Blanco: Investigation.
L. Extramiana: Investigation.
I. Lacave: Investigation.
G. Abizanda: Investigation.
E. Miranda: Investigation.
X. Agirre: Writing – review & editing.
F. Prósper: Writing – review & editing.
A. Pineda-Lucena: Writing – review & editing.
J. Pons-Villanueva: Conceptualization, Investigation, Writing – original draft, Writing – review & editing.
A. Pérez-Ruiz: Conceptualization, Investigation, Formal analysis, Writing – original draft, Writing – review & editing.
J. Pons-Villanueva and A. Pérez-Ruiz contributed equally to this work.

Funding statement

The authors disclose receipt of the following financial or material support for the research, authorship, and/or publication of this article: this work was supported by the Spanish Ministerio de Ciencia, Innovación y Universidades (Grant PID2020-113822RB-C22).

ICMJE COI statement

The authors affirm that they do not possess any conflicting interests. A. Pérez-Ruiz reports that research support was provided by the Spanish Ministerio de Ciencia, Innovacion y Universidades (grant number PID2020-113822RB-C22) for this study. F. Prósper reports that the article processing charges were funded by the Foundation for Applied Medical Research.

Data sharing

The data that support the findings for this study are available to other researchers from the corresponding author upon reasonable request.

Acknowledgements

We thank DSHB for the antibodies used in this study.

Ethical review statement

All animal procedures conducted in this study adhered to the European and Spanish ethical and legal regulations governing the use of animals in experimentation. The procedures carried out on the animals were approved and authorized under the animal ethical protocol number 039-18.

Open access funding

The open access fee for this article was self-funded.